A Deterministic Method to Identify Multiple Local Extrema for the AC Optimal Power Flow Problem

Dan Wu,† *Student Member, IEEE*, Daniel K. Molzahn,‡ *Member, IEEE*,
Bernard C. Lesieutre,† *Senior Member, IEEE*, and Krishnamurthy Dvijotham,* *Member, IEEE*

***Abstract*—This paper presents a deterministic approach to compute multiple local extrema for AC Optimal Power Flow (ACOPF) problems. An elliptical representation of the sphere-confined Fritz John conditions is constructed from a quadratic formulation of the ACOPF problem. Application of a branch tracing method to the elliptical formulation enables the calculation of multiple solutions. Further, a monotone search strategy enhances the computational efficiency of finding multiple local solutions with improved objective values. The proposed approach is first illustrated using two small examples with known feasible spaces. Then, four additional local solutions to a 39-bus system are found using the proposed approach.**

***Index Terms*—Optimal power flow, Fritz John conditions, Continuation methods**

I. Introduction

The optimal power flow (OPF) problem determines a minimum cost operating point that satisfies both physical constraints (i.e., the power flow equations) and engineering limits (e.g., voltage magnitude limits, line flow limits, and power generation limits). The full nonlinear OPF problem is referred to as the ACOPF, and a commonly used linearized version is called the DCOPF. Generically, an ACOPF problem is nonconvex [1], [2], may have multiple local solutions [3], [4], and is generally NP-Hard [5], [6].

Many nonlinear optimization algorithms have been applied to ACOPF problems, including Newton-Raphson iteration, sequential quadratic programming, penalty function methods, interior point methods, evolutionary algorithms, swarm algorithms, etc. [7]–[10]. Success of most algorithms only guarantees local optimality. As systems can have multiple local minima (see the examples in [3], [4]), there is a need for algorithms that search for globally optimal solutions and find multiple solutions in order to gain confidence in the best solution. Furthermore, there is interest in finding multiple optima and additional stationary points to characterize and better understand optimization problems [11]. As described in Section IV of [3] and in [11], the presence of saddle points or other stationary points may result in the failure of local algorithms to converge to local solutions.

With regard to pursuing optimality, recent convex relaxation approaches have shown success in obtaining the global solutions of some ACOPF problems. The first convex relaxation proposed was a second-order cone programming (SOCP) formulation in [12], with subsequent work including tighter semidefinite programming (SDP) formulations [13], [14]. Convex relaxations enclose the non-convex feasible space of the original OPF problem in a convex space. If the solution to the convex relaxation is feasible for the original non-convex problem, the relaxation is *exact* or, equivalently, has *zero relaxation gap*. While the SOCP and SDP relaxations are exact for certain test cases, they may fail to provide physically meaningful solutions to some problems [3], [15], [16]. Several sufficient conditions have been developed that guarantee exactness of various convex relaxations [17]. These conditions require certain topological structures and other non-trivial technical conditions that many problems fail to satisfy.

For cases where the relaxations of [12]–[14] are not exact, extensions include moment relaxation approaches [18]–[20]. These approaches generalize the SDP relaxation of [14] using the Lasserre hierarchy for polynomial optimization [21]. While this significantly increases the problem size, a sparse structure can be retained to improve tractability [22]. These approaches are promising, and research continues.

Another approach to achieve global optimality is to enumerate local solutions. Current approaches [3] find multiple local solutions of ACOPF problems by repeatedly executing local optimization algorithms with large numbers of random initializations. In this way, the authors of [3] demonstrated the ability to find multiple local optima for many system models. The global optima were found among the local solutions (as verified using convex relaxation techniques), and they made compelling arguments about properties of the sub-optimal local minima. With some exceptions, they found that certain local algorithms are often able to locate the global optima when initialized from a flat start.

This paper aims to compute multiple local solutions to feasible instances of the ACOPF problem in a principled, deterministic manner.[1] The proposed approach computes stationary solutions to the first-order optimality conditions and then checks the second-order sufficient conditions [23] to identify local extrema. To find solutions to the first-order optimality conditions, we apply the branch tracing method of our previous work [24], which was published in [25] to locate all the real-valued solutions to power flow equations. (This algorithm appears earlier in the thesis [26].) The branch tracing method embeds the real solution set for a system of n

†: University of Wisconsin–Madison, Dept. of Electrical and Computer Engineering, dwu43@wisc.edu, lesieutre@wisc.edu; ‡: Argonne National Laboratory, Energy Systems Division, dmolzahn@anl.gov; ∗: Pacific Northwest National Laboratory, dj@pnnl.gov

[1]The proposed approach can be extended to a family of nonconvex optimization problems in addition to ACOPF. We specifically require the ability to represent the first-order optimality conditions in an elliptical form that will be discussed in Section IV.

polynomials in $\mathbb{R}^n$ into a set of 1-dimensional curves defined by $(n-1)$ polynomials. Tracing all of these 1-dimensional curves provides the entire set of real solutions.

By solely searching for *real* solutions, the branch tracing approach has significant computational advantages over conventional root-tracing methods that scale with an upper bound on the number of *complex* solutions to the nonlinear equations, such as Numerical Polynomial Homotopy Continuation [27], [28]. (See the comparison in [24].) These computational advantages come at the expense of potential *incompleteness* of the solution set. The completeness of the branch tracing approach [25] with respect to finding all real-valued power flow solutions was countered by a small example in [29].

Branch tracing is an effective approach for identifying multiple power flow solutions. In [24], we revised the original representation to construct an *elliptical* formulation for the power flow equations. The elliptical formulation represents the power flow equations as quadratic expressions with associated matrices that are positive definite (i.e., high-dimensional ellipses $x^T\mathbf{M}_i x = b_i$ with $\mathbf{M}_i = \mathbf{M}_i^T$ positive definite and $b_i > 0$). The principle advantage of this representation is that all branch traces of the elliptical formulation are *bounded*, which is not the case for general quadratic polynomials.

Applying the branch tracing approach to the elliptical formulation of the power flow equations captures all the solutions of every existing case for which the solution set has been fully solved, including the counterexample in [29].[2] This paper extends this tracing approach from solving the power flow equations to ACOPF problems by constructing an elliptical formulation of the first-order optimality conditions of ACOPF problems and then tracing 1-dimensional curves to locate multiple local solutions.

This deterministic method offers an alternative algorithm for finding multiple local optima. As in other research, notably [3], the results can be used to find the best optimum by enumeration, especially when an SDP fails to do so, and for the purpose of examining properties of local minima. The proposed algorithm confirms some of the results in [3] with regard to local minima. Additionally, the algorithm also locates local maxima and saddle points which may further enhance understanding of the properties of these systems. (For example, in [11] it is argued that the complexity of a problem can be inferred from the saddle points.) Note that the tracing methods can be computationally intensive. At this point, the proposed algorithm is particularly well-suited for research purposes. For instance, application to one of the modified 39-bus systems from [4] yields four new local minima in addition to the previously reported three, as well as thousands of saddle points, that are not easily found using traditional methods.

The paper is organized as follows. Section II introduces the quadratic model of the ACOPF problem. Section III discusses drawbacks of the Karush-Kuhn-Tucker (KKT) optimality conditions for our purposes and introduces sphere-confined Fritz John (FJ) optimality conditions instead. Section IV constructs an elliptical form of the Fritz John conditions. Section V describes how to trace curves via the branch tracing method. Section VI first applies the proposed approach to two example problems with disconnected feasible spaces. The proposed approach finds all the reported local minima as well as the global minima for both problems. The proposed approach is then applied to a modified 39-bus system [4]. Section VII concludes the paper.

The contributions of this paper are summarized below.

1) Construction of an elliptical formulation for the first-order conditions of ACOPF problems.
2) Proposal of a deterministic method that can search for multiple local optima (which can include the global optima) for ACOPF problems, including cases where the feasible regions are disconnected and relaxation approaches fail to find optimal solutions.
3) Introduction of a monotone search strategy to enhance the search performance.
4) Identification of four new local minima in addition to the previously reported three local minima of a 39-bus test case.
5) Demonstration that a medium-size OPF problem can have thousands of stationary points.

II. Equality-Constrained AC OPF Model

Consider an electric power system with N_{bus} buses, N_{line} lines, N_{gen} generators, and N_{load} loads. Without loss of generality, suppose that the first to the N_{gen}-th buses are generator buses and the rest are load buses. Let $\mathbf{P}_{gen} \in \mathbb{R}^{N_{gen}}$ be the active power generation vector and $\mathbf{V} \in \mathbb{C}^{N_{bus}}$ be the complex voltage vector, the real part of which is $\mathbf{v}_d$ and the imaginary part of which is $\mathbf{v}_q$. Define the bus admittance matrix as $\mathbf{Y}_{bus} \in \mathbb{C}^{N_{bus}\times N_{bus}}$ with real and imaginary parts $\mathbf{Y}_{bus} = \mathbf{G}_{bus} + \mathbf{j}\mathbf{B}_{bus}$, where $\mathbf{j} = \sqrt{-1}$. Denote $\mathbf{I}_f \in \mathbb{C}^{N_{line}}$ as the current vector entering the transmission lines such that $\mathbf{I}_f = \mathbf{Y}_f\mathbf{V}$ and $\mathbf{I}_t \in \mathbb{C}^{N_{line}}$ as the current vector leaving the transmission lines such that $\mathbf{I}_t = \mathbf{Y}_t\mathbf{V}$. Denote $diag[\cdot]$ as the diagonalization operator. Let $\mathrm{Re}(\cdot)$ and $\mathrm{Im}(\cdot)$ denote the operators taking the real part and the imaginary part, respectively. Further define

$$
\begin{aligned}
O(\cdot) &=: \frac{1}{2}\begin{bmatrix} \mathrm{Re}(\cdot) & -\mathrm{Im}(\cdot) \\ \mathrm{Im}(\cdot) & \mathrm{Re}(\cdot) \end{bmatrix} && \text{(1a)}\\
\mathbf{u} &=: \begin{bmatrix} \mathbf{v}_d^T & \mathbf{v}_q^T \end{bmatrix}^T && \text{(1b)}\\
\mathbf{M}_{V,k} &=: diag\left[\mathbf{e}_k^T \ \mathbf{e}_k^T\right] && \text{(1c)}\\
\mathbf{M}_{I,j} &=: diag\left[\mathbf{t}_j^T \ \mathbf{t}_j^T\right] && \text{(1d)}\\
\mathbf{M}_{P,k} &=: \mathbf{M}_{V,k}O(\mathbf{Y}_{bus}) + O(\mathbf{Y}_{bus})^T\mathbf{M}_{V,k} && \text{(1e)}\\
\mathbf{M}_{Q,k} &=: \mathbf{M}_{V,k}O(\mathbf{j}\mathbf{Y}_{bus}) + O(\mathbf{j}\mathbf{Y}_{bus})^T\mathbf{M}_{V,k} && \text{(1f)}\\
\mathbf{M}_{f,j} &=: O(\mathbf{Y}_f)^T\mathbf{M}_{I,j}O(\mathbf{Y}_f) && \text{(1g)}\\
\mathbf{M}_{t,j} &=: O(\mathbf{Y}_t)^T\mathbf{M}_{I,j}O(\mathbf{Y}_t) && \text{(1h)}
\end{aligned}
$$

where $\mathbf{e}_k \in \mathbb{R}^{N_{bus}}$ is a column vector with a single unity element at the k-th entry and $\mathbf{t}_j \in \mathbb{R}^{N_{line}}$ is a column vector with a single unity element at the j-th entry.

Consider a cost function defined by a quadratic polynomial in terms of the active power generation. The OPF problem

[2]This indicates that the characteristics of the branch tracing approach depend on the problem formulation, which provides flexibility for improvements via problem reformulation. The elliptical reformulation has theoretical advantages (i.e., boundedness of the traces) and empirical results demonstrate an improved performance relative to the original formulation.

minimizes the cost function while satisfying constraints on active and reactive power balances, squared voltage magnitudes, squared line current flows, and generator outputs:

$$\textbf{Minimize} \quad J = \sum_{i=1}^{N_{gen}} d_i P_{gen,i}^2 + c_i P_{gen,i} \tag{2a}$$

Subject to:

$$\text{Gen. Balance:} \quad P_{gen,i} - P_{load,i} = \mathbf{u}^T \mathbf{M}_{P,i} \mathbf{u} \tag{2b}$$

$$\text{Load Balance:} \quad -P_{load,m} = \mathbf{u}^T \mathbf{M}_{P,m} \mathbf{u} \tag{2c}$$

$$-Q_{load,m} = \mathbf{u}^T \mathbf{M}_{Q,m} \mathbf{u} \tag{2d}$$

$$\text{Voltage Limit:} \quad \mathbf{u}^T \mathbf{M}_{V,k} \mathbf{u} \le V_{max,k}^2 \tag{2e}$$

$$-\mathbf{u}^T \mathbf{M}_{V,k} \mathbf{u} \le -V_{min,k}^2 \tag{2f}$$

$$\text{Gen. Limit:} \quad P_{gen,i} \le P_{max,i} \tag{2g}$$

$$-P_{gen,i} \le -P_{min,i} \tag{2h}$$

$$\mathbf{u}^T \mathbf{M}_{Q,i} \mathbf{u} \le Q_{max,i} \tag{2i}$$

$$-\mathbf{u}^T \mathbf{M}_{Q,i} \mathbf{u} \le -Q_{min,i} \tag{2j}$$

$$\text{Current Limit:} \quad \mathbf{u}^T \mathbf{M}_{f,j} \mathbf{u} \le I_{max,j}^2 \tag{2k}$$

$$\mathbf{u}^T \mathbf{M}_{t,j} \mathbf{u} \le I_{max,j}^2 \tag{2l}$$

$$\text{Index:} \quad i = 1, \ldots, N_{gen}$$

$$m = N_{gen}+1, \ldots, N_{bus}$$

$$k = 1, \ldots, N_{bus}$$

$$j = 1, \ldots, N_{line}$$

where d_i and c_i are constants, $P_{gen,i}$ is the i-th entry of $\mathbf{P}_{gen}$, $P_{load,i}$ is the active power demand at bus i, $Q_{load,m}$ is the reactive power demand at bus m, $V_{max,k}$ and $V_{min,k}$ are the upper and lower limits on voltage magnitude at bus k, $P_{max,i}$ and $P_{min,i}$ are the upper and lower limits on active power generation at bus i, $Q_{max,i}$ and $Q_{min,i}$ are the upper and lower limits on reactive power generation at bus i, and $I_{max,j}$ is the upper limit for both current entering and leaving line j.

Note that the decision variables in (2) are $\mathbf{P}_{gen}$ and $\mathbf{u}$.[3] Although (2b) can be substituted in (2a) and (2h) to eliminate $\mathbf{P}_{gen}$, doing so would induce a quartic cost function with respect to $\mathbf{u}$, which causes difficulties for constructing an elliptical formulation in Section IV. We therefore keep $\mathbf{P}_{gen}$ as an explicit variable in our formulation.

Although (2) employs line current flow limits, apparent power flow limits can also be integrated in our model via the introduction of $4N_{line}$ additional constraints. A detailed description of apparent power line flow limits is provided in Appendix I-A. The 39-bus system example in Section VI is simulated using apparent power line flow limits.

To convert (2) into equality-constrained model, we introduce unconstrained slack variables: $s_{Vmax,k}$, $s_{Vmin,k}$ for the voltage magnitude limits, $s_{Imax,f,j}$ and $s_{Imax,t,j}$ for the line current flow limits, and $s_{Qmax,i}$ and $s_{Qmin,i}$ for the reactive power limits. Specifically, the voltage limits (2e) and (2f) are reformulated as

$$\mathbf{u}^T \mathbf{M}_{V,k} \mathbf{u} + s_{Vmax,k}^2 = V_{max,k}^2 \tag{3a}$$

$$s_{Vmin,k}^2 - \mathbf{u}^T \mathbf{M}_{V,k} \mathbf{u} = -V_{min,k}^2. \tag{3b}$$

[3]To set an angle reference, remove the entry of v_q corresponding to the reference bus and delete the corresponding row and columns in (2).

The line current limits (2k) and (2l) are reformulated as

$$\mathbf{u}^T \mathbf{M}_{f,j} \mathbf{u} + s_{Imax,f,j}^2 = I_{max,j}^2 \tag{4a}$$

$$\mathbf{u}^T \mathbf{M}_{t,j} \mathbf{u} + s_{Imax,t,j}^2 = I_{max,j}^2. \tag{4b}$$

The reactive power limits (2i) and (2j) are reformulated as

$$\mathbf{u}^T \mathbf{M}_{Q,i} \mathbf{u} + s_{Qmax,i}^2 = Q_{max,i} \tag{5a}$$

$$s_{Qmin,i}^2 - \mathbf{u}^T \mathbf{M}_{Q,i} \mathbf{u} = -Q_{min,i}. \tag{5b}$$

However, to maintain a quadratic form, different treatments for active power generation and its bounds are employed due to different types of cost functions. We first assume that the active power generation is non-negative. This is usually the case for most generators since they are designed to deliver active power. If there are exceptions, a constant shift (adding the absolute value of the lower limit to both sides of active power generation inequalities) will provide an appropriate reformulation. Interested readers can refer to Appendix I-B for details.

If the cost function is linear, i.e., $J = \sum_{i=1}^{N_{gen}} c_i P_{gen,i}$, we define $p_{gen,i} =: \sqrt{P_{gen,i}}$. The active power generation limits are given by

$$p_{gen,i}^2 + s_{Pmax,i}^2 = P_{max,i} \tag{6a}$$

$$s_{Pmin,i}^2 - p_{gen,i}^2 = -P_{min,i} \tag{6b}$$

where $s_{Pmax,i}$ and $s_{Pmin,i}$ are unconstrained slack variables.

Thus, the equality-constrained ACOPF is

$$\textbf{Minimize} \quad J = \sum_{i=1}^{N_{gen}} c_i p_{gen,i}^2 \tag{7a}$$

Subject to:

$$\text{Gen. Balance:} \quad p_{gen,i}^2 - P_{load,i} = \mathbf{u}^T \mathbf{M}_{P,i} \mathbf{u} \tag{7b}$$

$$\text{Load Balance:} \quad -P_{load,m} = \mathbf{u}^T \mathbf{M}_{P,m} \mathbf{u} \tag{7c}$$

$$-Q_{load,m} = \mathbf{u}^T \mathbf{M}_{Q,m} \mathbf{u}$$

$$\text{Voltage Limit:} \quad \mathbf{u}^T \mathbf{M}_{V,k} \mathbf{u} + s_{Vmax,k}^2 = V_{max,k}^2 \tag{7d}$$

$$s_{Vmin,k}^2 - \mathbf{u}^T \mathbf{M}_{V,k} \mathbf{u} = -V_{min,k}^2$$

$$\text{Gen. Limit:} \quad p_{gen,i}^2 + s_{Pmax,i}^2 = P_{max,i} \tag{7e}$$

$$s_{Pmin,i}^2 - p_{gen,i}^2 = -P_{min,i}$$

$$\mathbf{u}^T \mathbf{M}_{Q,i} \mathbf{u} + s_{Qmax,i}^2 = Q_{max,i} \tag{7f}$$

$$s_{Qmin,i}^2 - \mathbf{u}^T \mathbf{M}_{Q,i} \mathbf{u} = -Q_{min,i}$$

$$\text{Current Limit:} \quad \mathbf{u}^T \mathbf{M}_{f,j} \mathbf{u} + s_{Imax,f,j}^2 = I_{max,j}^2 \tag{7g}$$

$$\mathbf{u}^T \mathbf{M}_{t,j} \mathbf{u} + s_{Imax,t,j}^2 = I_{max,j}^2$$

$$\text{Index:} \quad i = 1, \ldots, N_{gen}$$

$$m = N_{gen}+1, \ldots, N_{bus}$$

$$k = 1, \ldots, N_{bus}$$

$$j = 1, \ldots, N_{line}$$

If the cost function is quadratic, i.e., $J = \sum_{i=1}^{N_{gen}} d_i P_{gen,i}^2 + c_i P_{gen,i}$,[4] the active power generation limits (7e) are replaced by

$$P_{gen,i}^2 + s_{Pmax,i}^2 = P_{max,i}^2 \tag{8a}$$

[4]The cost function is not required to be convex; i.e., $d_i < 0$ is permissible.

$$s^2_{Pmin,i} - P^2_{gen,i} = -P^2_{min,i} \tag{8b}$$
$$p^2_{gen,i} - P_{gen,i} = 0 \tag{8c}$$

where $s_{Pmax,i}$ and $s_{Pmin,i}$ are unconstrained slack variables.

Then, the equality-constrained ACOPF formulation is

$$\textbf{Minimize} \quad J = \sum_{i=1}^{N_{gen}} d_i P^2_{gen,i} + c_i p^2_{gen,i} \tag{9a}$$

Subject to: (7b)**,** (7c)**,** (7d)**,** (7f)**,** (7g)**,** (8a)**,** (8b)**,** (8c) (9b)

III. First-Order Conditions in Quadratic Form

One way to solve an OPF problem is to compute its first-order optimality conditions. For example, consider the quadratic-cost ACOPF in (9). Note that the cost function and the constraints in (9) are all in quadratic form. Moreover, the constraints only have quadratic terms and constant terms except for (8c). (There are no linear terms in (7) since (8c) is intrinsically included in (7).) For notational convenience, the OPF problem (9) is succinctly written as

$$\begin{aligned} &\textbf{Minimize} && \mathbf{x}^T\mathbf{D}\mathbf{x} \\ &\textbf{Subject to}: && \mathbf{x}^T\mathbf{T}_j\mathbf{x} - r_j = 0 \\ &&& \mathbf{x}^T\mathbf{W}_i\mathbf{x} + \mathbf{b}_i^T\mathbf{x} - h_i = 0 \\ &&& j = 1, ..., N_q = 3N_{gen} + 4N_{bus} + 2N_{line} \\ &&& i = 1, ..., N_{gen} \end{aligned} \tag{10}$$

where $\mathbf{x}$ is the variable vector with dimension $N_v = 6N_{gen}+4N_{bus}+2N_{line}$ constructed by stacking $P_{gen,i}$, $p_{gen,i}$, $\mathbf{u}$, $s_{Pmax,k}$, $s_{Pmin,k}$, $s_{Qmax,k}$, $s_{Qmin,k}$, $s_{Vmax,k}$, $s_{Vmin,k}$, $s_{Imax,f,j}$ and $s_{Imax,t,j}$ into a column vector. The matrices $\mathbf{D}$, $\mathbf{T}_j$, $\mathbf{W}_i$, vectors $\mathbf{b}_i$ and scalars r_j and h_i correspond to the constraints in (9).

A. Challenges with the Karush-Kuhn-Tucker Conditions

The Lagrange function of the optimization problem (10) is

$$\begin{aligned} \mathcal{L}(\mathbf{x}, \lambda, \mu) = \quad & \mathbf{x}^T\mathbf{D}\mathbf{x} - \textstyle\sum_{j=1}^{N_q} \lambda_j\big(\mathbf{x}^T\mathbf{T}_j\mathbf{x} - r_j\big) \\ & - \textstyle\sum_{i=1}^{N_{gen}} \mu_i\big(\mathbf{x}^T\mathbf{W}_i\mathbf{x} + \mathbf{b}_i^T\mathbf{x} - h_i\big) \end{aligned} \tag{11}$$

where $\lambda \in \mathbb{R}^{N_q}$ and $\mu \in \mathbb{R}^{N_{gen}}$ are vectors of Lagrange multipliers [23].

If $\mathbf{x}_*$ is a local solution[5] to the original problem (2), then it is also a local solution to (10). If the Linear Independent Constraint Qualification (LICQ) condition [23] holds for the binding constraints (including the equality constraints) of (2), by the Karush-Kuhn-Tucker (KKT) Conditions [23], there exist λ_* and μ_* such that the following conditions are satisfied:

$$\bigtriangledown_{\mathbf{x}} \mathcal{L}(\mathbf{x}_*, \lambda_*, \mu_*) = \mathbf{0} \tag{12a}$$
$$\mathbf{x}_*^T\mathbf{T}_j\mathbf{x}_* - r_j = 0 \tag{12b}$$
$$\mathbf{x}_*^T\mathbf{W}_i\mathbf{x}_* + \mathbf{b}_i^T\mathbf{x}_* - h_i = 0 \tag{12c}$$
$$\lambda_a^* \le 0 \tag{12d}$$

where a is in the index set of the active inequality constraints of (2). Note that the complementarity conditions for the original OPF problem (2) are intrinsically included in (12a). Specifically, they are equivalent to the partial derivatives of $\mathcal{L}(\mathbf{x}, \lambda, \mu)$ with respect to the slack variables.

However, the KKT conditions lack some important features for constructing an elliptical formulation, and the dependence on constraint qualifications can cause difficulties for the branch tracing method. To understand these restrictions, we further examine (12a):

$$\begin{aligned} \bigtriangledown_{\mathbf{x}} \mathcal{L}(\mathbf{x}, \lambda, \mu) = \quad & 2\mathbf{D}\mathbf{x} - \textstyle\sum_{j=1}^{N_q} 2\lambda_j\mathbf{T}_j\mathbf{x} \\ & - \textstyle\sum_{i=1}^{N_{gen}} \mu_i\big(2\mathbf{W}_i\mathbf{x} + \mathbf{b}_i\big) = \mathbf{0}. \end{aligned} \tag{13}$$

Since λ and μ are unknowns when we solve the first-order conditions, (13) is quadratic with respect to $\mathbf{x}$, λ and μ, with some linear terms $\mathbf{D}\mathbf{x}$ and $\mu_i\mathbf{b}_i$. Since λ and μ only appear in the cross-product terms with $\mathbf{x}$, there are no univariate quadratic terms of λ or μ in (13). This makes it impossible to construct a positive-definite quadratic polynomial (i.e., an ellipse) as a linear combination of (12) with respect to $\mathbf{x}$, λ, and μ that retains the KKT solutions.

Another issue occurs from the strong reliance on the constraint qualifications. It is possible that an optimization problem has a solution that does not satisfy the constraint qualifications, which may result in the nonexistence of KKT solutions.[6] Since the branch tracing method that will be described in Section V traces through the first-order conditions by continuously changing certain parameters, our approach may reach points that fail to satisfy the constraint qualifications. Attempting to use the KKT conditions for our proposed tracing approach may therefore result in numerical issues.

B. The Sphere-Confined Fritz John Conditions

To deal with the difficulties associated with the KKT conditions, we introduce the Fritz John (FJ) conditions restricted to a sphere. A detailed comparison between the FJ conditions and the KKT conditions can be found in [30], and an application of FJ conditions to ACOPF problems can be found in [31]. Briefly, the FJ conditions are a generalized version of the KKT conditions which do not require the same constraint qualifications. However, the FJ conditions can induce "fictitious" local solutions [30], but this issue can be easily addressed as described in this section.

First, define a scalar function $\mathcal{F}(\mathbf{x}, \lambda, \mu, \delta)$:

$$\begin{aligned} \mathcal{F}(\mathbf{x}, \lambda, \mu, \delta) = \quad & \delta\mathbf{x}^T\mathbf{D}\mathbf{x} - \textstyle\sum_j \lambda_j\big(\mathbf{x}^T\mathbf{T}_j\mathbf{x} - r_j\big) \\ & - \textstyle\sum_i \mu_i\big(\mathbf{x}^T\mathbf{W}_i\mathbf{x} + \mathbf{b}_i^T\mathbf{x} - h_i\big) \end{aligned} \tag{14}$$

where δ is a scalar multiplier associated with the objective and λ and μ are the multiplier vectors for the constraints.

If $\mathbf{x}_*$ is a local solution to the original problem (2), then it is also a local solution to (10). By the Fritz John Conditions [30] for (2), there exist δ_*, λ_*, and μ_* such that

$$\bigtriangledown_{\mathbf{x}} \mathcal{F}(\mathbf{x}_*, \lambda_*, \mu_*, \delta_*) = \mathbf{0} \tag{15a}$$

[5]We use "local solution" to refer to a local minimum, "KKT solution" to denote a point that satisfies the KKT conditions, "Fritz John (FJ) solution" to indicate a point that satisfies the FJ conditions, and "stationary point" to mean a point that satisfies the equalities in either the KKT conditions or the FJ conditions, but does not necessarily satisfy the inequalities for the multipliers. Also, we use "saddle point" to refer a stationary point that is not a local extremum (i.e., neither a local maximum nor a local minimum).

[6]For instance, minimizing x subject to $x^2 = 0$ has the trivial solution $x = 0$, but no KKT solutions exist [30].

$$\mathbf{x}_*^T\mathbf{T}_j\mathbf{x}_* - r_j = 0 \tag{15b}$$
$$\mathbf{x}_*^T\mathbf{W}_i\mathbf{x}_* + \mathbf{b}_i^T\mathbf{x}_* - h_i = 0 \tag{15c}$$
$$(\delta_*, \lambda_*, \mu_*) \neq (0, \mathbf{0}, \mathbf{0}) \tag{15d}$$
$$\lambda_{*k} \leq 0, \text{ if } \delta_* \geq 0 \tag{15e}$$
$$\lambda_{*k} \geq 0, \text{ if } \delta_* \leq 0 \tag{15f}$$

where k is in the index set of the active inequality constraints of (2). Note that LICQ implies $\delta_* \neq 0$, in which case the FJ solution is also a KKT solution. Thus, one can easily check for fictitious solutions induced by the FJ conditions via examination of δ_*.

Consider (15a) in detail:

$$\begin{aligned}\bigtriangledown_{\mathbf{x}}\mathcal{F}(\mathbf{x}, \lambda, \mu, \delta) = \quad & 2\delta\mathbf{D}\mathbf{x} - \textstyle\sum_j 2\lambda_j\mathbf{T}_j\mathbf{x} \\ & - \textstyle\sum_i \mu_i\big(2\mathbf{W}_i\mathbf{x} + \mathbf{b}_i\big) = \mathbf{0}.\end{aligned} \tag{16}$$

If $\mathbf{x}_*$, δ_*, λ_*, and μ_* is a solution to (16), then $\mathbf{x}_*$, $K\delta_*$, $K\lambda_*$, and $K\mu_*$ is also a solution for any $K \neq 0$. To avoid infinitely many solutions, we regularize the non-zero condition (15d) with a sphere constraint on the multipliers:

$$\delta^2 + \lambda^T\lambda + \mu^T\mu = 1. \tag{17}$$

The sphere constraint results in univariate quadratic terms for all of the multipliers, which enables the construction of the elliptical formulation described in Section IV.

In summary, the sphere-confined Fritz John conditions are

$$\bigtriangledown_{\mathbf{x}}\mathcal{F}(\mathbf{x}_*, \lambda_*, \mu_*, \delta_*) = \mathbf{0} \tag{18a}$$
$$\mathbf{x}_*^T\mathbf{T}_j\mathbf{x}_* - r_j = 0 \tag{18b}$$
$$\mathbf{x}_*^T\mathbf{W}_i\mathbf{x}_* + \mathbf{b}_i^T\mathbf{x}_* - h_i = 0 \tag{18c}$$
$$\delta^2 + \lambda^T\lambda + \mu^T\mu = 1 \tag{18d}$$

where (15e) and (15f) are temporarily dropped here for the convenience of constructing the elliptical formulation and tracing the paths. These inequalities will be revisited to check for optimal solutions after solving (18).

IV. Elliptical Formulation of the Sphere-Confined Fritz John Conditions

This section applies a similar strategy to [24] to construct a high-dimensional elliptical representation of the FJ conditions for the ACOPF problem. To begin, define a set $\Omega \subset \mathbb{R}^N$ as an $(N-1)$-dimensional real ellipse centered at $\mathbf{x}_0$:

$$\Omega = \{\mathbf{x} \in \mathbb{R}^N | (\mathbf{x} - \mathbf{x}_0)^T\mathbf{H}(\mathbf{x} - \mathbf{x}_0) = 1, \mathbf{H} = \mathbf{H}^T, \mathbf{H} \succ 0\}$$

where $\succ 0$ denotes positive definiteness.

It is trivial to show that any $(N-1)$-dimensional real ellipse is a bounded, simply-connected, $(N-1)$-dimensional manifold. Converting every quadratic equation of (18) into a high-dimensional ellipse ensures the boundedness of the curves employed in the tracing method described in Section V and that these curves form closed loops.

With the preparation of Sections II and III, we are now able to represent the sphere-confined FJ conditions in an elliptical formulation. Our goal is to retain the solution set of (18) while converting the quadratic matrix of each equation of (18) to a positive-definite matrix. This can be done if one ellipse, called the *base ellipse*, can be constrcuted by a linear combination of the equations in (18). A base ellipse for the sphere-confined Fritz John conditions is

$$\begin{aligned}&\sum_{i=1}^{N_{gen}} \big[(P_{gen,i}^2 + s_{Pmax,i}^2 - P_{max,i}^2) + \frac{1}{2}(s_{Pmin,i}^2 \\ &\quad - P_{gen,i}^2 + P_{min,i}^2) + (\mathbf{u}^T\mathbf{M}_{Q,i}\mathbf{u} + s_{Qmax,i}^2 \\ &\quad - Q_{max,i}) + (s_{Qmin,i}^2 - \mathbf{u}^T\mathbf{M}_{Q,i}\mathbf{u} + Q_{min,i}) \\ &\quad + (p_{gen,i}^2 - P_{load,i} - \mathbf{u}^T\mathbf{M}_{P,i}\mathbf{u})\big] \\ &+ \sum_{j=1}^{N_{line}} \big[(\mathbf{u}^T\mathbf{M}_{f,j}\mathbf{u} + s_{Imax,f,j}^2 - I_{max,j}^2) \\ &\quad + (\mathbf{u}^T\mathbf{M}_{t,j}\mathbf{u} + s_{Imax,t,j}^2 - I_{max,j}^2)\big] \\ &+\gamma_0 \sum_{k=1}^{N_{bus}} \big[(\mathbf{u}^T\mathbf{M}_{V,k}\mathbf{u} + s_{Vmax,k}^2 - V_{max,k}^2) \\ &\quad + \frac{1}{2}(s_{Vmin,k}^2 - \mathbf{u}^T\mathbf{M}_{V,k}\mathbf{u} + V_{min,k}^2)\big] \\ &+ (\delta^2 + \lambda^T\lambda + \mu^T\mu - 1) = 0\end{aligned} \tag{19}$$

where $\gamma_0 \in \mathbb{R}$ is a constant. Notice that the diagonal elements of $\mathbf{M}_{V,k}$ dominate the cross-products of $\mathbf{u}$ for sufficiently large γ_0. Thus, the quadratic (19) is formed with an associated positive-definite matrix for a sufficiently large choice of γ_0. A more detailed discussion of (19) can be found in Appendix B.

We add a scaled version of the base ellipse (19) to the FJ conditions in (18) so that all resulting polynomials are high-dimensional ellipses. We then normalize the constant of each ellipse to one by scaling the ellipse with the reciprocal of the associated constant. The concise expression of the elliptical formulation for the FJ conditions is

$$\begin{aligned}q_1(\mathbf{x}) &= \mathbf{x}^T\mathbf{H}_1\mathbf{x} + \mathbf{b}_1^T\mathbf{x} - 1 = 0 \\ &\vdots \\ q_N(\mathbf{x}) &= \mathbf{x}^T\mathbf{H}_N\mathbf{x} + \mathbf{b}_N^T\mathbf{x} - 1 = 0\end{aligned} \tag{20}$$

where $N = N_q + N_{gen} + N_v + 1$ is the total number of polynomials in the FJ conditions, $\mathbf{x} \in \mathbb{R}^N$, and $\mathbf{H}_i \succ 0$ for $i = 1, \ldots, N$. For the ACOPF problem with quadratic generation cost (9), the number of non-zero vectors $\mathbf{b}_i$ is equal to N_{gen}. These vectors are all zero if the cost function is linear.

Solutions to (20) satisfy the FJ conditions and therefore correspond to potentially optimal points. Finding multiple solutions to (20) is a challenging task. A classical approach is to use Newton's method; however, success of Newton's method is strongly dependent on selecting an appropriate initialization, which is generally difficult. Other methods based on homotopy continuation are guaranteed to yield all solutions to polynomial systems [32], [33]. However, the computational effort for these methods scales exponentially with the number of variables, and these methods are therefore inappropriate, even for small systems. The branch tracing method that will be presented in the following section provides an alternative, more tractable approach for finding multiple solutions to (20).

V. Identifying Multiple Fritz John Solutions by the Branch Tracing Method

With an elliptical formulation of first-order conditions, we are prepared to apply the branch tracing method presented in

[24] to identify multiple solutions to the Fritz John conditions of the ACOPF problem.

A. Branch Tracing Method

The branch tracing method can be interpreted as a means of searching through a higher-dimensional real algebraic set to locate an embedded lower-dimensional real algebraic set. While increasing the dimensionality often complicates a real algebraic set, searching a higher-dimensional space can aid in identifying multiple 0-dimensional real solutions of a polynomial system. Consider a linearly independent polynomial system

$$\mathbf{F}_N(\mathbf{x}) = \{f_i(\mathbf{x}),\ \mathbf{x} \in \mathbb{R}^N,\ i = 1, 2, \cdots, N\}. \tag{21}$$

Generically, the real algebraic set of (21) consists of finitely many 0-dimensional isolated real solutions which are generally difficult to locate because they are discretely scattered in $\mathbb{R}^N$. To overcome this, we relax one polynomial, say, the N-th polynomial $f_N(\mathbf{x})$, and consider the remaining $N-1$ polynomials

$$\mathbf{F}_{N-1}(\mathbf{x}) = \{f_i(\mathbf{x}),\ \mathbf{x} \in \mathbb{R}^N,\ i = 1, 2, \cdots, N-1\}. \tag{22}$$

The real algebraic set of (22) is generically comprised of 1-dimensional curves in $\mathbb{R}^N$. These curves are almost everywhere smooth; moreover, they necessarily include the entire real algebraic set of (21). Thus, if the real algebraic set of (21) is 0-dimensional,[7] given a real solution of (21) and following the 1-dimensional curves via the branch tracing method can identify other real solutions of (21). Furthermore, if all the curves are bounded and connected to each other, this method provides the entire real solution set. The boundedness of the curves is guaranteed by the elliptical formulation in (20). The connectedness is still under investigation. Even without a theoretical guarantee for the connectedness at present, the numerical simulations in this paper and in [24] provide all the real solutions to the systems whose entire real solution sets were reported. Future work includes finding a sufficient condition for connectedness.

To locate solutions along 1-dimensional curves, we relax each ellipse in (20) individually. Specifically, we add one extra tracing variable α_i to the i-th equation of (20):

$$q_i(\mathbf{x}) = \alpha_i \tag{23a}$$
$$q_j(\mathbf{x}) = 0 \qquad \forall j \neq i \tag{23b}$$

In practice, a predictor-corrector algorithm is applied to follow the traces. A trace terminates upon returning to its initial point. Interested readers can find specific details about predictor-corrector implementations in [34].

Given a feasible OPF problem and a known FJ solution as a starting point, the enumeration search strategy described in Algorithm 1 (as well as the following monotone search strategy) may produce additional FJ solutions.

[7]The assumption of a generic problem is not confining in practice. An arbitrarily small perturbation of the problem can reduce the non-generic case to a generic one, resulting in a 0-dimensional solution set. Such a perturbation is not restrictive for any practical problems since every parameter value in the problem is not exact but rather approximated.

Algorithm 1 Enumeration Search Strategy

1: **procedure** OBTAIN A STARTING POINT
Choose a starting point which is in a current solution set of (20) but has not yet been traced. The initial starting point is obtained from any suitable local algorithm.

2: **procedure** TRACE PATHS
At the starting point, apply the branch tracing method to the elliptical formulation of the FJ conditions to trace paths of $\mathbf{x}$ formed by continuously and individually changing each α_i. Each trace terminates upon returning to the starting point. Parallel computation can be used to trace the paths associated with each α_i.

3: **procedure** UPDATE SOLUTION SET
Record stationary points (at which $\alpha_i = 0$) encountered on the paths and compare them to the current solution set. Update the solution set by adding newly found solutions which are distinct from the existing solutions.

4: **procedure** TERMINATION
If every point in the solution set has been traced or a solution has an objective value that is sufficiently close to the lower bound obtained from a convex relaxation, output the best solution. Otherwise, return to 1.

The number of the traces N_{trace} required for enumerating real solutions is bounded by

$$N_{trace} \leq N_{real} \times N \tag{24}$$

where N_{real} denotes the number of the real solutions to the FJ conditions and N is the number of the equations. However, estimating a sharp bound for the number of real solutions N_{real} to a polynomial system itself is a hard problem. A comprehensive introduction to this topic can be found in [35]. For power system models, special structures appear to limit the number of real solutions. As observed in [24], [25], for example, the numbers of real solutions to power flow problems seem to be far less than their estimated upper bounds. However, no validated theoretical results can be found at present to explain this large discrepancy. Some empirical results indicate that the number of solutions may be related to the network topology [36].

The computational complexity for following one trace is heavily dependent on the corrector step of predictor–corrector algorithm. The corrector step is performed using Newton's method, which requires the solution of multiple linear systems. A naïve implementation could use LU decomposition, which has a complexity of $O(n^3)$ if a dense matrix size is $n \times n$. A more sophisticated implementation could exploit the sparsity of the Jacobian matrix. The complexity of the corresponding sparse solver depends on specific network structure. Also note that the sparsity pattern of the Jacobian matrix for a given OPF problem is the same for every trace computed in the proposed algorithm. Thus, the symbolic factorization step used by a sparse solver only needs to be performed once, which can further improve computational tractability. Future work includes implementing more sophisticated sparse solution techniques.

Algorithm 1 begins with a starting point. For this we rely on decades of algorithmic development to find a single starting solution. Steps 2 and 3 in Algorithm 1 compute traces and perform bookkeeping to collect solutions. For each solution found by Algorithm 1, traces for all equations are computed without duplication (i.e., if more than one solution lies on the same trace, the trace is only computed once).

With the solution set returned, we can compare the objective function values to locate the best solution. In the absence of a sufficient condition for connectedness of the traces, the solution set is not guaranteed to contain the global optimum. However, the best solution in the resulting set will clearly have an objective function value that is at least as good as that from the initial starting point. Further, the numerical examples in Section VI demonstrate that the proposed approach can find the global solutions to challenging problems, and some of the global solutions obtained by the proposed approach significantly improve on the initial starting points obtained from a local solver.

The proposed approach is synergistic with both local algorithms and convex relaxation techniques. Local solution algorithms are needed to obtain an initial starting point for the proposed algorithm.[8] When searching for the global optimum, the tracing can be concluded upon obtaining a local solution with an objective value that is sufficiently close to the *termination criterion* provided by the lower bound from a convex relaxation, e.g., [12]–[14], [17]–[20], [22]. Additionally, we emphasize that the traces also find local maxima and saddle points that may be of interest to researchers.

B. Monotone Search Strategy

The tracing strategy in Algorithm 1 follows at most $N_{real} \times N$ traces before terminating. However, if we are only interested in the global solution, or at least a better solution than the initial starting point, then a more efficient search strategy can be applied. Specifically, a "monotone search strategy" introduces one extra constraint using the objective function to the ACOPF problem in (7) or (9).

Suppose we have a known solution $(\mathbf{P}_{gen,*},\ \mathbf{u}_*)$ to the first-order conditions of (9). At this solution, the objective function value is $J_* = \sum_{i=1}^{N_{gen}} d_i P_{gen,i,*}^2 + c_i p_{gen,i,*}^2$. Using this value, we enforce the constraint

$$\sum_{i=1}^{N_{gen}} d_i P_{gen,i}^2 + c_i p_{gen,i}^2 + \tau^2 = J_* + \epsilon^2 \qquad (25)$$

where τ is a free slack variable and ϵ is a small constant.

Since $\tau^2 \geq 0$, the objective function is confined to be less than $J_* + \epsilon^2$. The value of J_* is updated upon finding a better solution (i.e., a lower objective value).[9] The monotone search strategy is provided in Algorithm 2. This strategy can significantly reduce the number of traces relative to the enumeration search strategy for locating a better solution, which is a key determinant of the computational tractability of the proposed approach.

Algorithm 2 Monotone Search Strategy

1: **procedure** OBTAIN AN INITIAL POINT
Begin with an initial starting point using any suitable local algorithm. Compute the threshold value J_* for the cost function at the starting point. Choose a small value for ϵ.

2: **procedure** TRACE PATHS
Apply the branch tracing method to the elliptical formulation of the FJ conditions of (7) or (9) augmented by (25). Specifically, trace the paths of $(\mathbf{x},\ \tau)$ by continuously and individually changing each α_i. If a solution $(\mathbf{x}_*,\ \tau_*)$ with $|\tau_*| \geq \epsilon$ is found while tracing a certain path, stop tracing the rest, set $(\mathbf{x}_*,\ \tau_*)$ as a new starting point, compute the corresponding J_* value, and re-start from the first path.

3: **procedure** TERMINATION
If every path has been traced with no solution satisfying $|\tau_*| \geq \epsilon$, terminate and output the latest starting point.

Note that the monotone search currently has no guarantee of finding the best solution achievable with Algorithm 1. Although a monotone path to the global optima always exists in our simulations, it is possible that the global solution is only connected to the stationary points that have higher objective values than the starting point. Developing sufficient conditions that prevent this situation is a direction for future research.

VI. NUMERICAL EXAMPLES

This section provides several examples for which the proposed approach yields multiple local minima and the global optima but the SDP relaxation of [14] is not exact. These examples were proposed and studied in [3] with random initial starting points to locate multiple local minima. See [4] for the test case data and the results from the approach of [3]. The feasible spaces of the 5-bus (WB5) and the 9-bus (case9mod) examples are investigated in [39] and shown to be disconnected. While many local algorithms cannot bridge disconnected feasible spaces to search for multiple solutions, our proposed approach finds all local minima and the global optima for these two problems. Moreover, we also report seven local minima (including the global minimum) to the 39-bus (case39mod4) example, which include four new local minima in addition to the three reported in [3], [4].

Our tracing program was coded in Matlab and executed on a PC with a 2.8GHz Intel i-7 CPU and 4GB RAM for the 5- and 9-bus systems. The initial conditions are solved by MATPOWER 5.0 [37] with MIPS solver under default settings. We do not explore the effect of different initialization in this paper. An incomplete enumeration for the 39-bus system was performed in parallel using the compute resources and assistance of the Center for High Throughput Computing (CHTC) at the University of Wisconsin–Madison Department

[8] Appropriate local solution algorithms include interior point methods [8], [37] or the feasible point pursuit-successive convex approximation approach [38]. The latter approach claims a guarantee of finding a KKT point, which is particularly relevant for initializing our tracing algorithm.

[9] In our simulations, we set ϵ to be approximately 10% of the best-known objective value. This provides some flexibility for the traces to connect to higher-cost solutions before finding a lower-cost solution. However, this is unnecessary for the numeric examples tested so far; for each test case, the monotone search algorithm always finds a lower-cost solution from the previously-best-known solution.

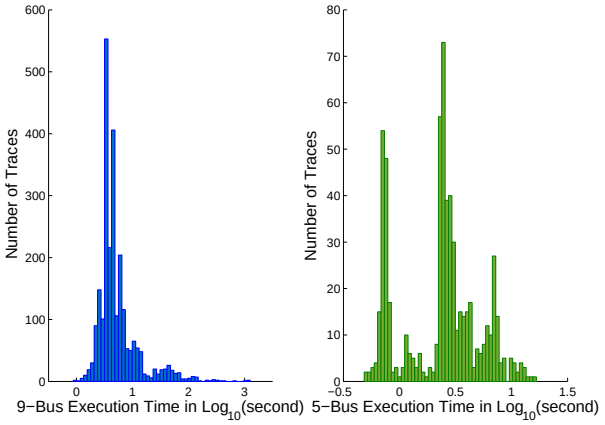

Fig. 1. Execution Time of Enumeration Strategy for case9mod (Left) and WB5 (Right)

of Computer Sciences. Each trace was assigned to an autonomous computer with one CPU, 2 GB of memory, and 4 GB of disk space.

A. 9-Bus System Example: "case9mod"

The first example is "case9mod" in [4]. This case has nine buses, nine transmission lines, and three generators with quadratic cost functions. Since neither current flow limits nor apparent power flow limits are binding for this case, both models will provide the same solutions. We chose to enforce current flow limits in accordance with (2) in order to obtain a smaller problem size.

The enumeration search strategy terminates after 2489 traces and returns 27 stationary solutions, among which four are verified to be local minima, five are local maxima, and the rest are saddle points. These four local minima, which are listed in Table I, match those in [4]. Solution 4 in the last column of Table I is the global optimum as verified both by exhaustive search of the feasible space [39] and by the second-order moment relaxation [18]. The overall execution time is 2.78×10^4 seconds (7.7 hours) with mean and median times for each trace of 11.2 seconds and 4.3 seconds, respectively. A histogram plot of the execution times for each trace (on a log scale) is shown in Fig. 1 on the left. Although the traces were computed sequentially, parallel computing techniques could be used to reduce the computation time. Note that most of the traces terminated within a few seconds, but a small fraction of the traces were much slower. Reasons for the slow traces include 1) many sharp corners on a trace resulting in a small step size, 2) many portions of the trace with poor numeric conditioning, which require careful numerical rescaling techniques, and 3) encountering many solutions which are indistinguishable except for a change in sign of the slack variables.

The monotone search strategy described in Section V-B is next applied to the same problem. Projections of the monotone search traces and solutions are depicted in Fig. 2. The gray regions in the Fig. 2 illustrate a projection of the disconnected feasible space generated using the method described in [39].

TABLE I
LOCAL MINIMA FOR CASE9MOD FROM THE ENUMERATION SEARCH

	Sol. 1	Sol. 2	Sol. 3	Sol. 4
$\|V_1\|$	0.9020	0.9027	0.9064	0.9095
$\|V_2\|$	0.9175	0.9169	0.9255	0.9218
$\|V_3\|$	0.9247	0.9272	0.9326	0.9388
$\|V_4\|$	0.9098	0.9104	0.9096	0.9127
$\|V_5\|$	0.9104	0.9120	0.9109	0.9160
$\|V_6\|$	0.9279	0.9307	0.9387	0.9426
$\|V_7\|$	0.9177	0.9182	0.9271	0.9284
$\|V_8\|$	0.9213	0.9204	0.9299	0.9291
$\|V_9\|$	0.9000	0.9000	0.9000	0.9000
θ_1	$0°$	$0°$	$0°$	$0°$
θ_2	$-9.304°$	$-11.555°$	$7.245°$	$12.367°$
θ_3	$-11.150°$	$-8.619°$	$12.115°$	$7.006°$
θ_4	$-5.770°$	$-5.722°$	$-0.400°$	$-0.398°$
θ_5	$-10.044°$	$-9.507°$	$0.219°$	$-0.732°$
θ_6	$-11.542°$	$-10.128°$	$7.592°$	$4.842°$
θ_7	$-12.855°$	$-12.884°$	$4.173°$	$4.516°$
θ_8	$-10.906°$	$-11.980°$	$4.548°$	$7.118°$
θ_9	$-10.383°$	$-10.722°$	$-1.511°$	$-0.631°$
S_1	$1.432-j0.05$	$1.422-j0.05$	$0.1-j0.05$	$0.1-j0.05$
S_2	$0.378-j0.05$	$0.100-j0.05$	$0.648-j0.05$	$1.254-j0.05$
S_3	$0.1-j0.05$	$0.388-j0.05$	$1.178-j0.05$	$0.570-j0.05$
Cost	4246.55	4265.04	3397.97	3087.89

$|V_i|\,\angle\theta_i$ and S_i denote the voltage and power injections at bus i in per unit. Costs are given in \$/hr.

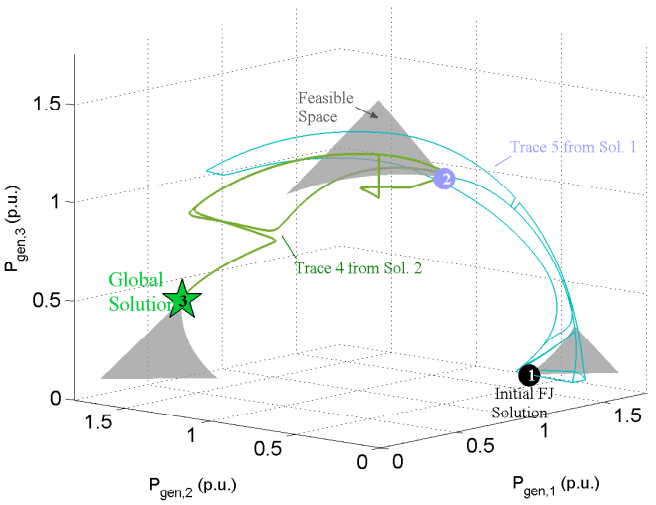

Fig. 2. Selected Monotone Search Traces for case9mod

Starting at an initial stationary point (black dot) obtained by MATPOWER 5.0 [37], the monotone search strategy locates the stationary point (light blue dot labeled 2) via the fifth trace (light blue curve). The fourth trace (green curve) starting from the second stationary point yields the global optimum (the green star labeled 3). The monotone search approach uses 9 traces to locate the global solution, which is significantly fewer than the 2489 traces used in the enumeration strategy. The overall execution time was 214.6 seconds with mean and median times for each trace of 23.8 seconds and 11.6 seconds, respectively. The overall execution time is thus 130 times faster than the full enumeration.

The monotone search solutions are listed in Table II. Observe that the objective function value is monotonically decreasing at each solution. Note also that the intermediate

TABLE II
FJ SOLUTIONS FOR CASE9MOD FROM THE MONOTONE SEARCH

	FJ Sol. 1	FJ Sol. 2	FJ Sol. 3
$\|V_1\|$	0.9020	0.9075	0.9095
$\|V_2\|$	0.9175	0.9178	0.9218
$\|V_3\|$	0.9247	0.9251	0.9388
$\|V_4\|$	0.9098	0.9107	0.9127
$\|V_5\|$	0.9104	0.9101	0.9160
$\|V_6\|$	0.9279	0.9304	0.9426
$\|V_7\|$	0.9177	0.9174	0.9284
$\|V_8\|$	0.9213	0.9211	0.9291
$\|V_9\|$	0.9000	0.9000	0.9000
θ_1	$0°$	$0°$	$0°$
θ_2	$-9.304°$	$-1.982°$	$12.367°$
θ_3	$-11.150°$	$8.511°$	$7.006°$
θ_4	$-5.770°$	$-2.151°$	$-0.398°$
θ_5	$-10.044°$	$-2.383°$	$-0.732°$
θ_6	$-11.542°$	$-3.506°$	$4.842°$
θ_7	$-12.855°$	$-1.614°$	$4.516°$
θ_8	$-10.906°$	$-2.409°$	$7.118°$
θ_9	$-10.383°$	$-5.080°$	$-0.631°$
S_1	$1.432-j0.05$	$0.538-j0.05$	$0.1-j0.05$
S_2	$0.378-j0.05$	$0.100-j0.05$	$1.254-j0.05$
S_3	$0.1-j0.05$	$1.281-j0.05$	$0.570-j0.05$
Cost	4246.55	3829.84	3087.89

$|V_i|\angle\theta_i$ and S_i denote the voltage and power injection at bus i in per unit. Costs are given in \$/hr.

non-increasing solutions obtained by the monotone search may not necessarily be local minima. For instance, the second stationary point in Table II is not a local minimum.

B. 5-Bus System Example: "WB5"

The second example, "WB5", has five buses, six transmission lines, and two generators [4]. As shown in Fig. 3, which was created using the approach in [39], the feasible space for this problem has two disconnected regions. The enumeration search strategy computes 628 traces to yield 12 stationary points, among which two are local minima matching those reported in [3]. The overall execution time was 1959 seconds with mean and median times for each trace of 3.1 seconds and 2.5 seconds, respectively, with the distribution shown in Fig. 1 on the right. The monotone search strategy locates the global solution in the eleventh trace from the initial starting point. Fig. 3 depicts all the stationary solutions identified by the enumeration strategy as well as one of the traces in the enumeration strategy that connects to the global solution.[10] The overall execution time was 44 seconds (a factor of 44 faster than the full enumeration) with mean and median times for each trace of 4.0 seconds and 3.0 seconds, respectively. The black dot is the initial FJ solution given by MATPOWER, the blue diamonds denote all the stationary points identified by enumeration, and the green star is the best solution identified by the enumeration approach. As verified both by exhaustive search of the feasible space [39] and by the second-order moment relaxation [18], the green star is the global optimum.

A modified version of this example is illustrated in Appendix C. While both "IPOPT" and "MIPS" solvers failed to locate the global solution from a flat start, the proposed tracing method yields the global optimum for the modified system.

[10]The trace shown in Fig. 3 connects the initial solution to the global solution, but does not connect all the stationary points found by other traces.

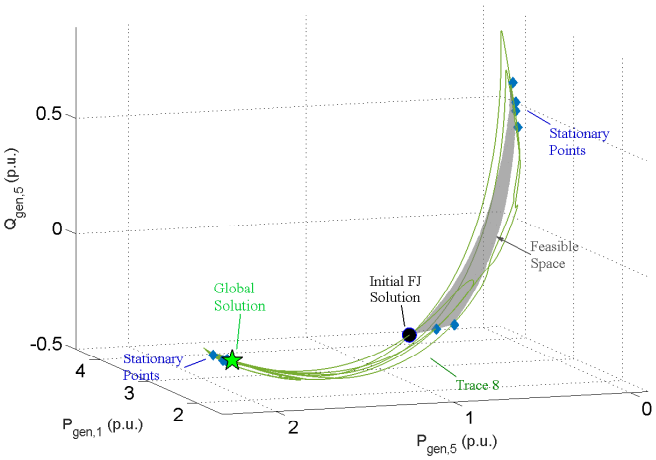

Fig. 3. Selected Enumeration Search Trace for WB5

C. 39-Bus System Example: "case39mod4"

This section considers a 39-bus system, "case39mod4", with 46 transmission lines and 10 generators. Three local minima have been reported for this system [4]. The proposed tracing method finds at least seven local minima (including the known three). The specific local minima are listed in Appendix D.

To make an exact comparison, we enforced apparent power flow limits on transmission lines (see Appendix A), which increases the number of variables from 556 to 924. Starting at the three known local minima, we computed a single trace of the paths associated with each constraint. This incomplete enumeration followed a total of 2772 paths to yield 10238 different stationary points, which included seven local minima (the three known local minima and four new ones) and six local maxima. Note that starting the enumeration algorithm from the second known local minimum yields six of the seven local minima (two known local minima and four new ones) using only 924 traces. Further investigation indicates that there exist over 3000 different concatenated paths[11] that connect every local minimum to the global minimum. The solutions found along some (but not all) of these concatenated paths have objective function values that are monotonically decreasing. Also note that despite the large number of stationary points, a concatenated path starting from a known local solution to the global solution can be simple. For example, a concatenated monotone path starting at a local minimum with cost 1068.30\$/hr passes through a saddle point with a lower cost of 866.80\$/hr, which then passes through another saddle point with a lower cost 567.64\$/hr and eventually reaches the global minimum with the lowest cost 557.14\$/hr. This monotonically decreasing path only passed through two additional intermediate stationary points to reach the global solution. Ongoing research includes developing methods for choosing which order to trace the paths such that low-cost solutions are obtained quickly.

[11]We use the phrase "concatenated path" to refer to the sequence of several individual paths concatenated at common solution points.

VII. Conclusion

This paper has proposed a deterministic approach to identify multiple local extrema of ACOPF problems. This approach introduces slack variables to convert the inequality-constrained ACOPF problem into an equality-constrained problem in quadratic form. Leveraging previous work for the power flow equations [24], the Fritz John optimality conditions are rewritten in an elliptical form. Applying a branch tracing method [25] to the elliptical formulation enables the computation of multiple solutions to the Fritz John optimality conditions for ACOPF problems, with the elliptical formulation ensuring boundedness of the traces. To improve computational performance, a monotone search strategy was proposed to reduce the number of traces used in locating the global solution. Three numerical examples illustrate the operation of our proposed approach. These examples demonstrate the approach's capability to identify multiple local extrema of ACOPF problems as well as locate the global optima. The first two examples show that the proposed approach can bridge multiple components of a disconnected feasible space to obtain the global solution. For the third example, the proposed tracing approach finds four new local optima beyond those reported in previous literature.

Future work will attempt to develop sufficient conditions that guarantee the connectedness of the 1-dimensional algebraic set of the elliptical formulation. Such conditions will ensure that the proposed approach yields the global solution. Other future work includes computational improvements, such as the exploitation of sparsity to solve larger problems.

While this paper focuses on ACOPF problems, elliptical formulations can be constructed for other classes of problems and the proposed approach thus has the potential to be applied more broadly. For instance, integer programs can be formulated with quadratic polynomial constraints (i.e., $x_i \in \{0, 1\}$ is equivalent to $x_i^2 - x_i = 0$). Integer programs with a small number of feasible points (thus potentially requiring few branch traces) may be good candidates for extending the applicability of the proposed approach.

Acknowledgement

The authors thank N.-J. Simon for help with display of the figures, and C. Koch and S. Goldstein for help with high throughput computing of CHTC. The authors gratefully acknowledge support from US DOE under Argonne National Laboratory subcontract 3F-30222, and the National Science Foundation under grant CNS1329452.

References

[1] I. Hiskens and R. Davy, "Exploring the Power Flow Solution Space Boundary," *IEEE Trans. Power Syst.*, vol. 16, no. 3, pp. 389–395, 2001.

[2] B. Lesieutre and I. A. Hiskens, "Convexity of the Set of Feasible Injections and Revenue Adequacy in FTR Markets," *IEEE Trans. Power Syst.*, vol. 20, pp. 1790–1798, Nov. 2005.

[3] W. Bukhsh, A. Grothey, K. McKinnon, and P. Trodden, "Local Solutions of the Optimal Power Flow Problem," *IEEE Trans. Power Syst.*, vol. 28, no. 4, pp. 4780–4788, 2013.

[4] W. Bukhsh, A. Grothey, K. McKinnon, and P. Trodden, "Test Case Archive of Optimal Power Flow (OPF) Problems with Local Optima." [Online]. Available http://www.maths.ed.ac.uk/optenergy/LocalOpt/, 2017.

[5] D. Bienstock and A. Verma, "Strong NP-hardness of AC Power Flows Feasibility," *arXiv:1512.07315*, Dec. 2015.

[6] K. Lehmann, A. Grastien, and P. Van Hentenryck, "AC-Feasibility on Tree Networks is NP-Hard," *IEEE Trans. Power Syst.*, vol. 31, pp. 798–801, Jan. 2016.

[7] J. Momoh, M. El-Hawary, and R. Adapa, "A Review of Selected Optimal Power Flow Literature to 1993. Part I: Nonlinear and Quadratic Programming Approaches," *IEEE Trans. Power Syst.*, vol. 14, no. 1, pp. 96–104, 1999.

[8] J. Momoh, M. El-Hawary, and R. Adapa, "A Review of Selected Optimal Power Flow Literature to 1993. Part II: Newton, Linear Programming and Interior Point Methods," *IEEE Trans. Power Syst.*, vol. 14, no. 1, pp. 105–111, 1999.

[9] Z. Qiu, G. Deconinck, and R. Belmans, "A Literature Survey of Optimal Power Flow Problems in the Electricity Market Context," in *Power Syst. Conf. Exposition (PSCE)*, pp. 1–6, IEEE, 2009.

[10] F. Capitanescu, "Critical Review of Recent Advances and Further Developments Needed in AC Optimal Power Flow," *Electric Power Sys. Res.*, vol. 136, pp. 57–68, 2016.

[11] Y. N. Dauphin, R. Pascanu, C. Gulcehre, K. Cho, S. Ganguli, and Y. Bengio, "Identifying and Attacking the Saddle Point Problem in High-Dimensional Non-Convex Optimization," in *Advances in Neural Information Processing Systems (NIPS)*, pp. 2933–2941, 2014.

[12] R. Jabr, "Radial Distribution Load Flow using Conic Programming," *IEEE Trans. Power Syst.*, vol. 21, no. 3, pp. 1458–1459, 2006.

[13] X. Bai, H. Wei, K. Fujisawa, and Y. Wang, "Semidefinite Programming for Optimal Power Flow Problems," *Int. J. Electr. Power & Energy Sys.*, vol. 30, no. 6, pp. 383–392, 2008.

[14] J. Lavaei and S. Low, "Zero Duality Gap in Optimal Power Flow Problem," *IEEE Trans. Power Syst.*, vol. 27, pp. 92–107, Feb. 2012.

[15] B. Lesieutre, D. Molzahn, A. Borden, and C. DeMarco, "Examining the Limits of the Application of Semidefinite Programming to Power Flow Problems," in *49th Ann. Allerton Conf. Commun., Control, Comput. (Allerton)*, pp. 1492–1499, 2011.

[16] D. Molzahn and I. Hiskens, "Convex Relaxations of Optimal Power Flow Problems: An Illustrative Example," *IEEE Trans. Circuits Syst. I: Reg. Papers*, vol. 63, pp. 650–660, May 2016.

[17] S. Low, "Convex Relaxation of Optimal Power Flow–Part II: Exactness," *IEEE Trans. Control Netw. Syst.*, vol. 1, no. 2, pp. 177–189, 2014.

[18] D. Molzahn and I. Hiskens, "Moment-Based Relaxation of the Optimal Power Flow Problem," *18th Power Syst. Comput. Conf. (PSCC)*, Aug. 2014.

[19] C. Josz, J. Maeght, P. Panciatici, and J. Gilbert, "Application of the Moment-SOS Approach to Global Optimization of the OPF Problem," *IEEE Trans. Power Syst.*, vol. 30, pp. 463–470, Jan. 2015.

[20] B. Ghaddar, J. Marecek, and M. Mevissen, "Optimal Power Flow as a Polynomial Optimization Problem," *IEEE Trans. Power Syst.*, vol. 31, pp. 539–546, Jan. 2016.

[21] J.-B. Lasserre, "Global Optimization with Polynomials and the Problem of Moments," *SIAM J. Optimiz.*, vol. 11, no. 3, pp. 796–817, 2001.

[22] D. Molzahn and I. Hiskens, "Sparsity-Exploiting Moment-Based Relaxations of the Optimal Power Flow Problem," *IEEE Trans. Power Syst.*, vol. 30, no. 6, pp. 3168–3180, 2015.

[23] J. Nocedal and S. Wright, "Numerical Optimization," Springer, 2nd ed., 2000.

[24] B. Lesieutre and D. Wu, "An Efficient Method to Locate All the Load Flow Solutions–Revisited," in *53rd Annu. Allerton Conf. Commun., Control, Comput. (Allerton)*, Sept. 2015.

[25] W. Ma and J. Thorp, "An Efficient Algorithm to Locate All the Load Flow Solutions," *IEEE Trans.Power Syst.*, vol. 8, no. 3, pp. 1077–1083, 1993.

[26] I. A. Hiskens, *Energy Functions, Transient Stability and Voltage Behavior in Power Systems*. PhD thesis, Electrical Engineering and Computer Science, The University of Newcastle, Australia, 1990.

[27] S. Guo and F. Salam, "Determining the Solutions of the Load Flow of Power Systems: Theoretical Results and Computer Implementation," in *IEEE 29th Ann. Conf. Decis. Contr. (CDC)*, pp. 1561–1566, Dec. 1990.

[28] D. Mehta, H. D. Nguyen, and K. Turitsyn, "Numerical polynomial homotopy continuation method to locate all the power flow solutions," *IET Generation, Transmission & Distribution*, vol. 10, no. 12, pp. 2972–2980, 2016.

[29] D. Molzahn, B. Lesieutre, and H. Chen, "Counterexample to a Continuation-Based Algorithm for Finding All Power Flow Solutions," *IEEE Trans. Power Syst.*, vol. 28, no. 1, pp. 564–565, 2013.

[30] M. Bazaraa, H. Sherali, and C. Shetty, *Nonlinear Programming: Theory and Algorithms*. Wiley, 3rd ed., 2006.

[31] K. Almeida and A. Kocholik, "Solving Ill-Posed Optimal Power Flow Problems Via Fritz-John Optimality Conditions," to appear in *IEEE Trans. Power Syst.*, 2016.

[32] F. Drexler, "A Homotopy Method for the Calculation of All Zeros of Zero-Dimensional Polynomial Ideals," *Develop. Stat.*, vol. 1, pp. 69–93, 1978.

[33] C. Garcia and W. Zangwill, "Determining All Solutions to Certain Systems of Nonlinear Equations," *Math. Oper. Res.*, vol. 4, no. 1, pp. 1–14, 1979.

[34] R. Seydel, *Practical Bifurcation and Stability Analysis*, vol. 5. Springer Science & Business Media, 2009.

[35] F. Sottile, *Real Solutions to Equations from Geometry*, vol. 57. American Mathematical Society Providence, RI, 2011.

[36] D. Molzahn, D. Mehta, and M. Niemerg, "Toward Topologically Based Upper Bounds on the Number of Power Flow Solutions," in *American Control Conference (ACC)*, July 6-8 2016.

[37] R. Zimmerman and C. Murillo-Sanchez and R. Thomas, "MATPOWER: Steady-State Operations, Planning and Analysis Tools for Power Systems Research and Education," *IEEE Trans. Power Syst.*, vol. 26, pp. 12–19, Feb. 2011.

[38] A. S. Zamzam, N. D. Sidiropoulos, and E. Dall'Anese, "Beyond Relaxation and Newton-Raphson: Solving AC OPF for Multi-Phase Systems with Renewables," to appear in *IEEE Trans. Smart Grid*.

[39] D. K. Molzahn, "Computing the feasible spaces of optimal power flow problems," *IEEE Transactions on Power Systems*, 2017.

APPENDIX A
LINE AND GENERATOR MODELING

This appendix explains how to model the apparent power line flow limits and active generation constraints with negative lower bounds.

A. Apparent Power Line Flow Limits

Define connection matrices $\mathbf{C}_f$ and $\mathbf{C}_t \in \mathbb{R}^{N_{line} \times N_{bus}}$ for lines and buses, respectively. The (j,k)-th entry of $\mathbf{C}_f$ is 1 if the j-th line is connected to the k-th "from" bus and the (j,r)-th entry of $\mathbf{C}_t$ is 1 if the j-th line is connected to the r-th "to" bus. Further, define

$$\mathbf{T}_{f,j} =: \mathbf{C}_f^T(j,:)\ \mathrm{conj}(\mathbf{Y}_f(j,:)) \tag{26a}$$
$$\mathbf{T}_{t,j} =: \mathbf{C}_t^T(j,:)\ \mathrm{conj}(\mathbf{Y}_t(j,:)) \tag{26b}$$
$$\mathbf{M}_{Pline,f,j} =: O(\mathbf{T}_{f,j} + \mathbf{T}_{f,j}^T) \tag{26c}$$
$$\mathbf{M}_{Qline,f,j} =: O(j\mathbf{T}_{f,j} + j\mathbf{T}_{f,j}^T) \tag{26d}$$
$$\mathbf{M}_{Pline,t,j} =: O(\mathbf{T}_{t,j} + \mathbf{T}_{t,j}^T) \tag{26e}$$
$$\mathbf{M}_{Qline,t,j} =: O(j\mathbf{T}_{t,j} + j\mathbf{T}_{t,j}^T) \tag{26f}$$

where $\mathbf{C}_f(j,:)$ is the j-th row of $\mathbf{C}_f$, $\mathbf{Y}_f(j,:)$ is the j-th row of $\mathbf{Y}_f$, and $\mathrm{conj}\,(\cdot)$ is the complex conjugate.

Limits on apparent power flows are formulated as

$$P_{line,f,j} = \mathbf{u}^T\mathbf{M}_{Pline,f,j}\mathbf{u} \tag{27a}$$
$$Q_{line,f,j} = \mathbf{u}^T\mathbf{M}_{Qline,f,j}\mathbf{u} \tag{27b}$$
$$P_{line,f,j}^2 + Q_{line,f,j}^2 \leq S_{max,j}^2 \tag{27c}$$
$$P_{line,t,j} = \mathbf{u}^T\mathbf{M}_{Pline,t,j}\mathbf{u} \tag{27d}$$
$$Q_{line,t,j} = \mathbf{u}^T\mathbf{M}_{Qline,t,j}\mathbf{u} \tag{27e}$$
$$P_{line,t,j}^2 + Q_{line,t,j}^2 \leq S_{max,j}^2 \tag{27f}$$

where P denotes active power; Q denotes reactive power; S denotes apparent power; subscripts "f" and "t" denote the "from" and "to" terminals, respectively; and subscript "j" indicates the line index.

One can replace (2k) and (2l) with (27) to formulate the ACOPF problem with flow limits in terms of apparent power. This adds $4N_{line}$ constraints to the problem.

B. Active Power Generation with a Negative Lower Bound

Consider (2h) with $P_{min,i} < 0$. This is equivalent to

$$0 \leq P_{gen,i} - P_{min,i} \leq P_{max,i} - P_{min,i} \tag{28}$$

If the cost function is linear, then we let $p_{gen,i}^2 =: P_{gen,i} - P_{min,i}$. Hence, (7b) can be written as

$$p_{gen,i}^2 - \hat{P}_{load,i} = \mathbf{u}^T\mathbf{M}_{P,i}\mathbf{u} \tag{29}$$

where $\hat{P}_{load,i} = P_{load,i} - P_{min,i}$ is a constant.

The cost function (7a) can be expressed as

$$J = \sum_{i=1}^{N_{gen}} c_i p_{gen,i}^2 + C \tag{30}$$

where $C = \sum_{i=1}^{N_{gen}} c_i P_{min,i}$ is a constant.

If the cost function is quadratic, we let $\hat{P}_{gen,i} =: P_{gen,i} - P_{min,i}$ and $p_{gen,i}^2 =: \hat{P}_{gen,i}$. Thus, the cost function is

$$J = \sum_{i=1}^{N_{gen}} d_i P_{gen,i}^2 + c_i P_{gen,i} \tag{31a}$$
$$= \sum_{i=1}^{N_{gen}} d_i(\hat{P}_{gen,i} + P_{min,i})^2 + c_i(\hat{P}_{gen,i} + P_{min,i}) \tag{31b}$$
$$= \sum_{i=1}^{N_{gen}} d_i\hat{P}_{gen,i}^2 + e_i\hat{P}_{gen,i} + a_i \tag{31c}$$
$$= \sum_{i=1}^{N_{gen}} d_i\hat{P}_{gen,i}^2 + e_i p_{gen,i}^2 + a_i \tag{31d}$$

where $e_i = 2d_iP_{min,i} + c_i$ and $a_i = d_iP_{min,i}^2 + c_iP_{min,i}$ are constants.

APPENDIX B
DISCUSSION OF THE BASE ELLIPSE

This appendix serves as a complementary document to further discuss the structure of the base ellipse in (19). However, one should note that the construction of the base ellipse is not unique. This paper provides a particular construction for simplicity. Other varieties may have different structures.

A basic principal to construct a base ellipse is to combine the quadratic terms of all the variables into one equation. It is not necessary to combine all the constraints to achieve this. For example, in (18) associated with problem (9), the decision variables include $P_{gen,i}$, $p_{gen,i}$, $\mathbf{u}$, $s_{Pmax,k}$, $s_{Pmin,k}$, $s_{Qmax,k}$, $s_{Qmin,k}$, $s_{Vmax,k}$, $s_{Vmin,k}$, and $s_{Imax,f,j}$, $s_{Imax,t,j}$ as well as the multipliers δ, λ, and μ. Thus, a selected set of equations, for example, (7b), (7d), (7f), (7g), (8a), (8b) and (18d), is enough to include the quadratic terms of all the variables. The base ellipse given by (19) is comprised of these equations with appropriate scaling factors.

To see why (19) represents a high-dimensional ellipse, arrange this equation as

$$\sum_{i=1}^{N_{gen}}(\frac{1}{2}P_{gen,i}^2+s_{Pmax,i}^2+\frac{1}{2}s_{Pmin,i}^2+s_{Qmax,i}^2$$
$$+s_{Qmin,i}^2+p_{gen,i}^2)+\sum_{j=1}^{N_{line}}(s_{Imax,f,j}^2+s_{Imax,t,j}^2)$$
$$+\gamma_0\sum_{k=1}^{N_{bus}}(s_{Vmax,k}^2+\frac{1}{2}s_{Vmin,k}^2)+\delta^2+\lambda^T\lambda+\mu^T\mu$$
$$+\mathbf{u}^T\big[\sum_{k=1}^{N_{bus}}\frac{\gamma_0}{2}\mathbf{M}_{V,k}+\sum_{j=1}^{N_{line}}(\mathbf{M}_{f,j}+\mathbf{M}_{t,j})-\sum_{i=1}^{N_{gen}}\mathbf{M}_{P,i}\big]\mathbf{u}$$
$$=\sum_{i=1}^{N_{gen}}(P_{max,i}^2-\frac{1}{2}P_{min,i}^2+Q_{max,i}-Q_{min,i}+P_{load,i})$$
$$+\sum_{j=1}^{N_{line}}2I_{max,j}^2+\gamma_0\sum_{k=1}^{N_{bus}}(V_{max,k}^2-\frac{1}{2}V_{min,k}^2)+1 \qquad (32)$$

where the constant terms are moved to the right hand side.

Note that every decision variable in (32) has a positive univariate quadratic term, but only the voltage variable $\mathbf{u}$ has cross-products. To ensure a positive-definite matrix, the positive univariate quadratic terms of the voltage variables must dominate the cross-products. This can be achieved by scaling $\sum_{k=1}^{N_{bus}}\mathbf{M}_{V,k}$ with a positive constant γ_0. Since $\sum_{k=1}^{N_{bus}}\mathbf{M}_{V,k}$ forms a sub-identity matrix associated with the voltage variables $\mathbf{u}$, a large enough γ_0 will result in the full matrix being positive definite. On the other hand, since $\sum_{k=1}^{N_{bus}}(V_{max,k}^2-\frac{1}{2}V_{min,k}^2)>0$, a large enough γ_0 ensures a positive constant term on the right hand side of (32). Therefore, (32) represents a high-dimensional ellipse. The choice of γ_0 usually depends on the smallest eigenvalue of $\sum_j(\mathbf{M}_{f,j}+\mathbf{M}_{t,j})-\sum_i\mathbf{M}_{P,i}$. In our simulations, γ_0 was chosen to be slightly greater than the absolute value of the smallest eignevalue, which was usually less than 40 in practice.

The elliptical formulation of the ACOPF problem can be generalized to an arbitrary quadratically constrained quadratic programming (QCQP) problem provided that the problem's feasible space is bounded. This can easily be shown by introducing fictitious constraints. Specifically, given a bounded QCQP problem, one can always introduce large fictitious bounds on the square of each decision variable as long as these bounds are never binding. Formulating these bounds as equalities using squared slack variables enables the construction of a base ellipse, which can further be used to convert every equality into the form of an ellipse.

APPENDIX C
APPLICATION TO A MODIFIED FIVE-BUS SYSTEM

We present a modified version of "WB5" system called "WB5mod". In contrast to IPOPT and MIPS, the proposed tracing algorithm finds the global optimum for this problem. The test case WB5mod has the following variations from WB5 in [4]:

- Bus voltage magnitude limits are $[0.9, 1.1]$,
- The generator at bus 1 has active power limits of $[2, 15]$ per unit and reactive power limits of $[0.4, 18]$ per unit,
- The generator at bus 5 has active power limits of $[0, 20]$ per unit and reactive power limits of $[8, -0.5]$ per unit,
- The cost function is $J = P_{gen,1}^2 + 2P_{gen,1} + 12P_{gen,5}^2 + 1200P_{gen,5}$.

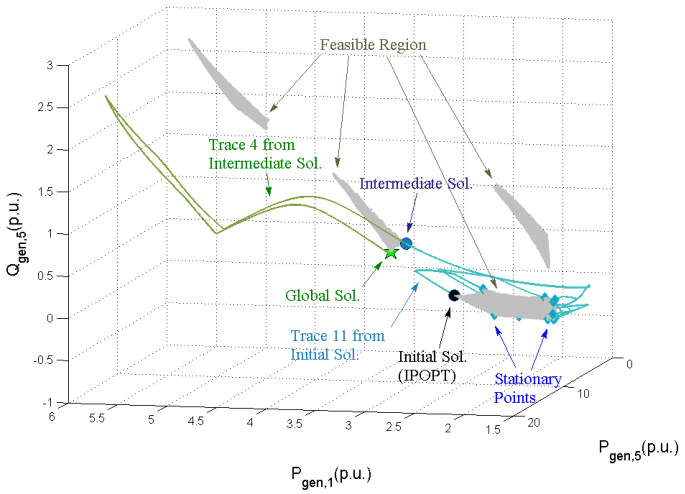

Fig. 4. Feasible Space and Selected Traces for WB5mod

When initialized from a flat start, both MIPS and IPOPT converged to a local solution with cost 161921.15 \$/hr. The proposed tracing algorithm found the global solution with a cost of 139875.00 \$/hr. (See Table III.) Note that the angle differences between adjacent buses are less than 30° for both solutions, despite the fact that these solutions are in different disconnected regions of the feasible space.

TABLE III
IPOPT SOLUTION, INTERMEDIATE STATIONARY POINT AND GLOBAL SOLUTION FOR WB5MOD

	IPOPT Sol.	Intermediate Sol.	Global Sol.
$\lvert V_1\rvert$	1.1000	0.9881	1.0892
$\lvert V_2\rvert$	1.03202	0.9053	1.0098
$\lvert V_3\rvert$	1.0255	0.9000	1.0045
$\lvert V_4\rvert$	0.9000	0.9000	0.9000
$\lvert V_5\rvert$	0.9232	0.9461	0.9358
θ_1	0°	0°	0°
θ_2	−6.8867°	−10.1765°	−8.6595°
θ_3	−7.0106°	−10.5328°	−8.9542°
θ_4	−15.3728°	−38.0141°	−36.5139°
θ_5	−11.5972°	−36.1330°	−34.9495°
S_1	$3.074+j0.4$	$3.5709+j0.4047$	$3.73+j0.4$
S_5	$0.3982-j0.299$	$0.1651+j0.2840$	$0+j0.1785$
Cost	161921.15	151310.41	139875.00

$\lvert V_i\rvert\angle\theta_i$ and S_i denote the voltage and power injection at bus i in per unit. Costs are given in \$/hr.

Fig. 4 shows the feasible region for this example as well as selected paths that connect the starting point to the global solution. The black dot represents the starting point found by IPOPT. A trace initialized from this point connects to an intermediate stationary point depicted by the blue dot, which is not a local minimum. Another trace connects this intermediate stationary point to the global solution at the green star.

APPENDIX D
ADDITIONAL LOCAL MINIMA FOR A 39-BUS SYSTEM

We list four new local minima for the example "case39mod4" in Table IV.

TABLE IV
NEW LOCAL MINIMA TO CASE39MOD4: BUS VOLTAGE & POWER INJECTION

	Sol. # 1		Sol. # 2		Sol. # 3		Sol. # 4	
Bus #	$\|V_1\|$	δ°	$\|V_1\|$	δ°	$\|V_1\|$	δ°	$\|V_1\|$	δ°
1	1.0381	-7.7180	1.0407	-8.8822	1.0381	-8.3789	1.0414	-9.7286
2	10500	-13.6302	1.0500	-13.9056	1.0500	-14.5736	1.0500	-14.8025
3	1.0311	-14.3376	1.0301	-14.2221	1.0318	-14.7228	1.0308	-14.5328
4	1.0164	-12.9683	1.0158	-12.8135	1.0176	-12.9721	1.0172	-12.7766
5	1.0171	-10.7174	1.0171	-10.7211	1.0182	-10.7163	1.0184	-10.7173
6	1.0178	-10.2212	1.0178	-10.2211	1.0189	-10.2100	1.0191	-10.2076
7	1.0141	-10.8564	1.0145	-10.9631	1.0152	-10.8776	1.0159	-11.0022
8	1.0141	-10.8809	1.0146	-11.0416	1.0152	-10.9191	1.0160	-11.1080
9	1.0338	-6.4855	1.0364	-7.5748	1.0348	-6.7911	1.0379	-8.0887
10	1.0269	-11.3978	1.0264	-11.2401	1.0283	-11.2899	1.0281	-11.1044
11	1.0234	-11.0195	1.0231	-10.9123	1.0247	-10.9427	1.0247	-10.8160
12	1.0203	-11.4129	1.0198	-11.2552	1.0217	-11.3049	1.0215	-11.1195
13	1.0239	-11.7426	1.0233	-11.5344	1.0255	-11.6035	1.0251	-11.3594
14	1.0182	-12.6373	1.0171	-12.2983	1.0200	-12.4170	1.0192	-12.0209
15	1.0027	-14.0066	0.9996	-13.0677	1.0058	-13.2255	1.0032	-12.1547
16	1.0020	-13.7728	0.9981	-12.5641	1.0056	-12.7498	1.0024	-11.3771
17	1.0148	-14.4987	1.0117	-13.8149	1.0157	-14.4508	1.0127	-13.6434
18	1.0208	-14.6582	1.0185	-14.2112	1.0217	-14.7768	1.0193	-14.2087
19	1.0080	-17.6118	1.0068	-16.4359	1.0108	-10.9482	1.0099	-9.5788
20	0.9500	-20.5983	0.9500	-19.4292	0.9500	-9.4907	0.9500	-8.1227
21	0.9836	-10.1557	0.9781	-8.0968	0.9894	-10.5188	0.9853	-8.2832
22	0.9760	-5.1747	0.9713	-2.1926	0.9807	-7.0300	0.9776	-3.8677
23	0.9720	-4.7886	0.9664	-2.1269	0.9777	-6.1090	0.9738	-3.2773
24	0.9989	-12.9764	0.9942	-11.5725	1.0036	-12.2741	0.9998	-10.7015
25	1.0383	-14.3653	1.0375	-14.6704	1.0332	-15.6994	1.0325	-15.9161
26	1.0312	-15.2774	1.0294	-15.7300	1.0263	-18.0348	1.0238	-18.2826
27	1.0221	-15.5262	1.0196	-15.4763	1.0196	-17.0044	1.0166	-16.7739
28	1.0147	-14.8419	1.0131	-16.2208	1.0079	-20.7534	1.0060	-21.8038
29	1.0052	-13.7943	1.0036	-15.4733	0.9980	-20.7266	0.9966	-22.0356
30	1.0486	-13.6302	1.0486	-13.9056	1.0486	-14.5736	1.0486	-14.8025
31	0.9500	0	0.9500	0	0.9500	0	0.9500	0
32	0.9900	-11.3978	0.9896	-11.2401	0.9913	-11.2899	0.9911	-11.1044
33	0.9500	-17.6357	0.9500	-16.4630	0.9500	-10.9642	0.9500	-9.5974
34	0.9552	-20.6398	0.9566	-19.4751	0.9552	-3.6968	0.9563	-2.3393
35	0.9500	-0.3855	0.9500	4.0725	0.9500	-4.6879	0.9500	-0.0062
36	0.9611	4.9342	0.9552	7.7125	0.9670	3.4967	0.9630	6.4074
37	1.0130	-14.2653	1.0122	-14.6704	1.0080	-15.6994	1.0074	-15.9161
38	0.9575	-10.8805	0.9558	-13.2279	0.9500	-20.0854	0.9500	-21.9683
39	1.0213	-3.3572	1.02442	-5.0848	1.0217	-3.8438	1.0253	-5.9033
Gen. #	P	Q	P	Q	P	Q	P	Q
1	0	1.4000	0	1.4000	0	1.4000	0	1.4000
2	6.46	0.5511	6.46	0.5507	6.4600	0.5113	6.4600	0.5027
3	0	1.5000	0	1.5000	0	1.5000	0	1.5000
4	0	0.5339	0	0.6054	0	0.3568	0	0.4153
5	0	0.7243	0	0.8012	5.0800	0.7255	5.0800	0.7868
6	5.2816	0.0734	6.8700	0.5351	2.5976	-0.3985	4.2670	-0.1056
7	5.8000	0	5.800	0	5.8000	0	5.8000	0
8	0	0	0	0	0	0	0	0
9	2.9827	-1.5000	2.2734	-1.5000	0.5882	-1.4680	0	-1.3570
10	11.0000	-1.0000	10.1394	-1.0000	11.0000	-1.0000	9.9438	-1.0000
Cost \$/hr	841.74066		848.92950		842.81718		847.54988	

Bus power injections are in per unit with a base power of 100 MVA.

Dan Wu (S'14) received the B.E. degree in electrical engineering and automation from the Huazhong University of Science and Technology, Wuhan, China, in 2012, and the M.S. degree from the University of Wisconsin-Madison, Madison, WI, USA, in 2014, where he is pursuing his Ph.D. degree in electrical engineering. His research interests include optimization theory and applications, electric power system analysis, information encryption techniques, and complex system theory.

Daniel K. Molzahn (S'09-M'13) is a Computational Engineer in the Energy Systems Division at Argonne National Laboratory. He was a Dow Postdoctoral Fellow in Sustainability at the University of Michigan, Ann Arbor and received the B.S., M.S., and Ph.D. degrees in electrical engineering and the Masters of Public Affairs degree from the University of Wisconsin–Madison, where he was a National Science Foundation Graduate Research Fellow. His research focuses on optimization and control of electric power systems.

Bernard Lesieutre (S'86 - M'93 - SM'06) received the B.S., M.S., and Ph.D. degrees in electrical engineering from the University of Illinois at Urbana-Champaign, Urbana, IL, USA. He is a Professor of Electrical and Computer Engineering at the University of Wisconsin-Madison, Madison, WI, USA. His research interests include the modeling, monitoring, and analysis of electric power systems and electric energy markets.

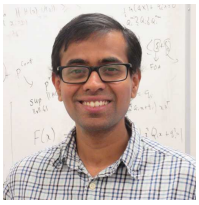

Krishnamurthy Dvijotham is a research engineer at Pacific Northwest National Laboratory (PNNL) in the advanced controls team. He was previously a postdoctoral fellow at the Center for Mathematics of Information at Caltech. He received his PhD in computer science and engineering from the University of Washington, Seattle in 2014 and a bachelors from IIT Bombay in 2008. His research interests span stochastic control theory, artificial intelligence, machine learning and markets/economics, and his work is motivated primarily by problems arising in large-scale infrastructure systems like the power grid. His research has won awards at several conferences in optimization, AI and machine learning.